JACS
JOURNAL OF THE AMERICAN CHEMICAL SOCIETY

Communication

pubs.acs.org/JACS

One-Pot in Situ Fabrication of Stable Nanocaterpillars Directly from Polyacetylene Diblock Copolymers Synthesized by Mild Ring-Opening Metathesis Polymerization

Ki-Young Yoon,[†] In-Hwan Lee,[†] Kyung Oh Kim,[†] Jihoon Jang,[‡] Eunji Lee,[‡] and Tae-Lim Choi*[,†]

[†]Department of Chemistry, Seoul National University, Seoul 151-747, Korea

[‡]Graduate School of Analytical Science and Technology, Chungnam National University, Daejeon 305-764, Korea

Supporting Information

ABSTRACT: We report a direct one-pot route for the preparation of supramolecules from simple polyacetylene diblock copolymers synthesized by mild ring-opening metathesis polymerization of cyclooctatetraene. This in situ nanoparticlization of conjugated polymer (INCP) approach is advantageous over conventional self-assembly processes because this method does not require any tedious postsynthetic treatments. Also, this direct approach provides intriguing supramolecules with a unique nanostructure resembling a caterpillar. Furthermore, the new supramolecules are highly stable adducts because the polyacetylene core block provides an exceptionally strong driving force for the self-assembly. Even though pristine polyacetylene is unstable in air, the polyacetylene segment in the nanocaterpillar is very stable because it is protected within the shell of the supramolecule.

Recent advances in the self-assembly of block copolymers (BCPs) in solution have enabled access to various intriguing nanostructures, such as undulated cylinders,[1] disklike micelles,[2] multicompartment structures,[3] and crystallization-driven self-assemblies.[4] However, all of these BCP self-assemblies inevitably require various additional postsynthetic processes such as redissolution in selective solvents,[1d] dialysis,[1b] change in temperature,[5] aging,[4c] chemical modification, or introduction of glue molecules,[1a] whereas nature provides more complex nanostructures in much simpler manners. These time-consuming postsynthesis treatments are necessary because the synthesis of the polymers does not guarantee a sufficiently strong driving force for their self-assembly. This problem was partially resolved by in situ self-assembly of amphiphilic BCPs, termed polymerization-induced self-assembly.[6] Nevertheless, these supramolecules are not thermodynamically stable adducts because the driving force holding the unimers of BCPs together is not strong enough. For this reason, small changes in solvent, temperature, or concentration would easily alter the nanostructures or even break the self-assembly. Therefore, another chemical postfunctionalization process to produce further cross-linking of either the core or the shell is required to obtain stable adducts.[1d] If stable supramolecules could be prepared directly by means of a simple one-pot procedure under mild conditions without any postsynthesis modification, even the large-scale production of nanostructured polymers would be possible.

Polyacetylene (PA) has attracted significant attention from both chemists and physicists because of its interesting electronic properties.[7] For this reason, various synthetic methods have been developed, such as Ziegler–Natta polymerization of acetylene,[7a] ring-opening metathesis polymerization (ROMP) of cyclooctatetraene (COT),[8] the Durham method,[9a] ROMP of benzvelene,[9b] and the use of poly(phenylvinyl sulfoxide) precursors.[9c] However, the synthesis and applications of PA are still challenging because of its instability in air and insolubility in *any* solvents, which arise from the strong $\pi-\pi$ interactions of the conjugated backbone. Chemists have tried to overcome the solubility challenge by preparing BCPs consisting of a soluble block and a PA block,[9c,10] mostly via indirect syntheses that require temperatures above 100 °C for the thermal elimination of certain leaving groups from PA.[11]

Even though ROMP of COT is the simplest way to synthesize PA, block copolymerization via this direct method has been only partially successful[10] because during ROMP of COT under dilute conditions[8a] or at elevated temperatures,[10a] an undesirable side reaction occurs that releases a large amount of benzene (over 50% based on consumed COT) and greatly lowers the conversion to PA (Scheme 1). Therefore, if a method to enhance COT conversion by suppressing benzene formation under mild conditions could be developed, ROMP would become the best method for the synthesis of BCPs containing a PA block. Herein we report a simple and direct ROMP of COT for the synthesis of soluble and stable PA

Scheme 1. ROMP of COT and Benzene Formation

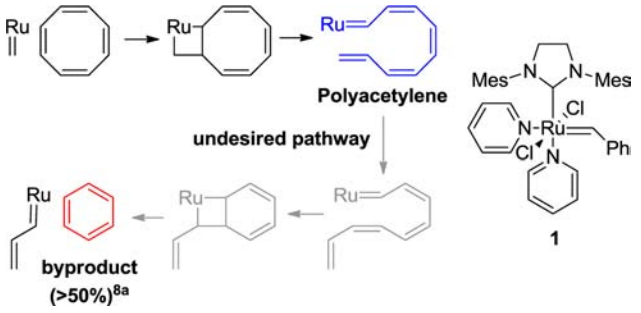

Received: May 28, 2012
Published: August 24, 2012

   dx.doi.org/10.1021/ja305150c | *J. Am. Chem. Soc.* 2012, 134, 14291–14294

BCPs. Through the use of a powerful and fast-initiating catalyst, benzene formation is greatly reduced. Notably, the resulting diblock copolymer spontaneously forms highly stable supramolecules with a unique caterpillar structure (nanocaterpillars) containing the conjugated PA core via the process called in situ nanoparticlization of conjugated polymer (INCP).

To synthesize well-defined diblock copolymers containing a long PA block, we used the highly active and fast-initiating third-generation Grubbs catalyst **1** for the ROMP of COT. **1** is ideal for the direct synthesis of diblock copolymers[12] because ROMP of low-strained COT (2.5 kcal/mol)[8b] is possible only with highly active catalysts. Moreover, fast initiation is crucial for the BCP synthesis. In addition, this highly active catalyst might promote the ROMP even at room temperature, which would suppress the formation of benzene, the major problem in previous reports.[8a,10a] To prepare a soluble PA BCP, a solubilizing first block was prepared by living ROMP of norbornene monomer **2**. After 20 min, COT was added at room temperature. The solution color immediately changed to red, implying that the conjugated polymer, PA, was being synthesized. To investigate the ROMP of COT, the polymerization was monitored in various deuterated solvents in a closed system, and the conversion of COT and the production of benzene were directly measured by ^{1}H NMR analysis (Table 1). From these experiments, we observed that the solvent

Table 1. Synthesis of the PA Diblock Copolymer by ROMP of COT

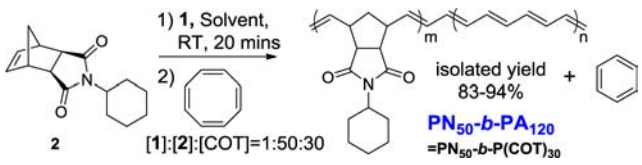

entry	solvent	conc (mM)[a]	time (h)	conv (%)	PhH (%)[b]	DP_{COT}[c]
1	THF	100	16	85	23	~20
2	toluene	100	16	77	17	~19
3	DCM	100	16	93	12	~25
4	DCM	10	16	73	32	~15
5	DCM	700	16	>99	9	~28

[a]Based on [COT]. [b]Yield of benzene formation calculated on the basis of the total number of double bonds from the converted COTs. [c]Degree of polymerization of COT (see the SI for details).

affected the COT conversion as well as the amount of benzene formation, and dichloromethane (DCM) was found to be the best solvent. In all cases, the percentage of benzene formation was much lower than in previous reports,[8a] confirming that the ROMP strategy at room temperature was indeed successful. The reaction concentration proved to be another determining factor, as ROMP of COT at a higher concentration resulted in higher conversion of COT and less benzene formation, while ROMP at a lower concentration gave the worst result (Table 1, entries 3−5). After the reaction was quenched by addition of ethyl vinyl ether, the polymer was purified by simple precipitation into MeOH.

Various in-depth characterizations of the resulting polymer were performed to confirm its chemical structure. Although the polymer was completely soluble in various organic solvents such as tetrahydrofuran (THF), toluene, and chloroform, liquid ^{1}H NMR analysis of the final polymer revealed only peaks corresponding to the polynorbornene (PN) block [Figure S1 in the Supporting Information (SI)]. The dark-red solution was analyzed by UV/vis spectroscopy, which revealed a spectrum with λ_{max} = 535 nm and two sets of distinguishable onset points at 630 and 800 nm (Figure 1). These two onset points

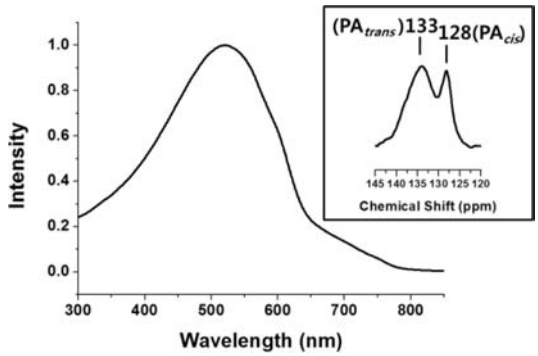

Figure 1. UV/vis spectrum in chloroform and (inset) CP-MAS ^{13}C solid-state NMR spectrum of PN_{50}-*b*-PA_{120}.

translated into band gaps of 2.0 and 1.6 eV, respectively, in perfect agreement with the band gaps for *cis*-PA and *trans*-PA, respectively.[13] Solid-state characterization provided further evidence for the presence of the PA block. In the elemental analysis, in comparison with the results for the PN homopolymer, additional carbon and hydrogen corresponding to PA were detected. From estimated calculations, an average of 28 COT units (or PA_{112}) were contained in PN_{50}-*b*-PA_{120} (Table S1 in the SI), in good agreement with the data in Table 1, entry 5. The microstructure of the PA block was further confirmed by cross-polarization/magic-angle-spinning (CP/MAS) ^{13}C solid-state NMR spectroscopy. The homopolymer of **2** showed only a single peak (132 ppm) in the C=C double bond region, whereas PN_{50}-*b*-PA_{120} showed additional peaks corresponding to both *cis*-PA (128 ppm) and *trans*-PA (133 ppm) (Figure 1 inset).[8b] Furthermore, cyclic voltammetry (CV) also revealed that two oxidation potentials for the diblock copolymer were related to the highest occupied molecular orbitals (HOMOs) of *cis*-PA (−5.49 eV) and *trans*-PA (−5.19 eV) (Figure S2). The much deeper HOMO of PN_{50}-*b*-PA_{120} relative to pristine PA (−4.5 to −4.2 eV),[14] is indicative of the improved stability of PN_{50}-*b*-PA_{120} in air, allowing for all of the characterizations in the ambient atmosphere. From these characterizations, we verified the integrity of the second PA block, which comprised polyenes with a mixture of *E* and *Z* stereoisomers, and this direct synthesis under mild conditions was the key to obtaining the PA block copolymer with high purity.

The observation that liquid NMR spectroscopy showed signals only for the PN block led us to investigate the self-assembly behavior of PN-*b*-PA. Since the growth of the insoluble second PA block during the copolymerization would promote the in situ formation of core−shell supramolecular structures, the core consisting of $\pi-\pi$-stacked PA would not appear in the liquid NMR analysis (Figure S1). The formation of supramolecules was also supported by size-exclusion chromatography (SEC) analysis eluted by THF.[15] SEC analysis of PN_{50}-*b*-PA_{40} ([COT] = 10) showed two distinguished traces at 274 and 12 kDa. The major peak at 274 kDa indicated the self-assembled aggregates of PN_{50}-*b*-PA_{40}, whereas the minor peak at 12 kDa corresponded to single chains of PN_{50}-*b*-PA_{40} containing relatively shorter PA chains, which were dis-

dx.doi.org/10.1021/ja305150c | J. Am. Chem. Soc. 2012, 134, 14291−14294

assembled as a result of the shear pressure under the SEC conditions (see Figure S3 for details).[15] X-ray diffraction analysis showed a signal at 0.34 nm on average (Figure S4), implying that the $\pi-\pi$ interaction within the PA core blocks was very strong and these supramolecular adducts were stable enough to maintain the self-assembly under the shear pressure of the SEC conditions. Thus, this in situ supramolecular formation did not require any additional processes to induce self-assembly.

Detailed information on the nanostructure was obtained by atomic force microscopy (AFM). Spin-coating of a dilute chloroform solution of PN_{50}-*b*-PA_{40} onto mica revealed spherical nanostructures having a diameter of 31 nm and a height of 2 nm with a highly uniform size distribution (Figure 2a). As the PA block was lengthened from 10 to 50 equiv of

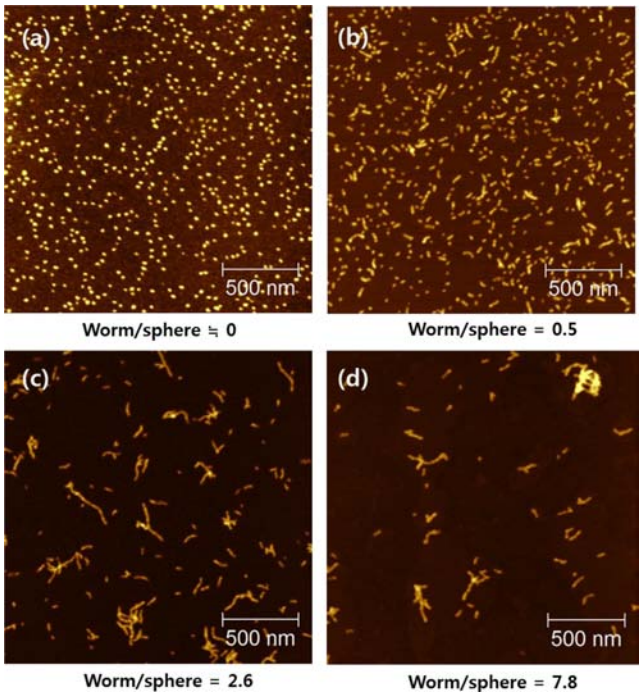

Figure 2. AFM images of the nanostructures self-assembled on mica from PN-*b*-PA obtained using [**2**]:[COT] ratios of (a) 50:10, (b) 50:20, (c) 50:30, and (d) 50:50.

COT, the heights and hydrodynamic volumes of the supramolecules increased (Figure S5), and structural evolution was observed as the PA block lengthened. For PN_{50}-*b*-PA_{80}, some portion of the nanospheres began to transform into wormlike micelles (Figure 2b), and the ratio of the populations of the wormlike and spherical micelles increased (0.5, 2.6, and 7.8; Figure 2b–d) as the amount of COT increased. Even though the wormlike micelles were as long as 500 nm (Figure 2d), 11% of the supramolecules were still spheres. We believe that because of polydispersity in the PA block, these spheres in Figure 2c,d contained PA cores with an insufficient block size (Figures S3 and S5), preventing them from transforming into wormlike micelles.

Surprisingly, high-resolution AFM images of PN_{50}-*b*-PA_{120} revealed the obtained wormlike structure to be very different from the ordinary ones. The magnified image (Figure 3a inset) clearly shows a highly undulated supramolecule resembling a caterpillar. The side-view image also supports the formation of supramolecules interconnected by the spheres (Figure 3b).

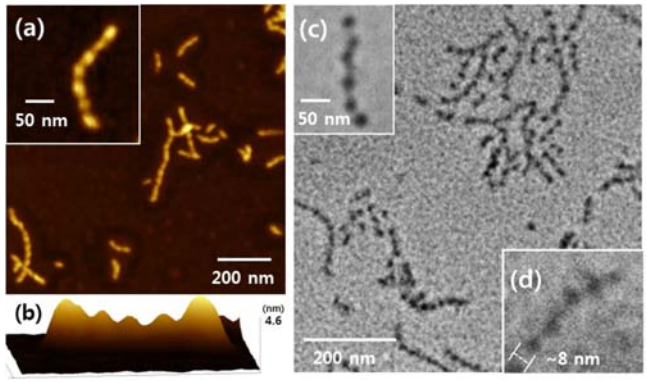

Figure 3. (a) AFM images of the nanocaterpillar structures from PN_{50}-*b*-PA_{120}s on mica substrate. (b) AFM 3D side-view image. (c) TEM images of the nanocaterpillar structures on a carbon-coated copper grid. (d) Cryo-TEM image in chloroform.

More insights into the structure of this intriguing supramolecule were obtained by transmission electron microscopy (TEM) analysis, where no staining with the sample was necessary because the electron density difference between the PN shell and electron-rich PA core provided sufficient contrast for TEM imaging. Magnified images revealed that despite existing as one supramolecule, the PA cores were not connected at all (Figure 3c). Nevertheless, these nanocaterpillar structures were surprisingly stable, as the integrity of the nanostructure was still maintained even when the polymer solution was heated at 100 °C for 20 min or the sample was sonicated for 30 min right before the spin-coating for AFM imaging. These results further demonstrate that the supramolecular adducts are thermodynamically stable under heating and mechanical and shear forces.

In addition to the solid-state imaging, further structural information on PN_{50}-*b*-PA_{120} in solution was obtained using cryogenic TEM (cryo-TEM) and dynamic light scattering (DLS). The cryo-TEM images vividly showed the presence of the same nanocaterpillars containing PA cores with an average diameter of 8 nm (Figure 3d and Figure S6), confirming the unique nanostructure in the solution state as well. In addition, the DLS analysis in chloroform revealed two distinct populations with average hydrodynamic diameters of 17 nm (minor) and 104 nm (major) (Figure S7a). This also proved the coexistence of the nanocaterpillars (104 nm) and the smaller nanospheres (17 nm) in solution, as already observed in the AFM and TEM images (Figure 3). Furthermore, when DLS analysis was conducted at high temperature up to 90 °C and after sonication, the sizes and distribution of the nanostructures were still maintained (Figure S7b–d). All these observations led to the conclusion that the diblock copolymers spontaneously self-assembled into highly stable nanocaterpillars in solution without any additional postsynthetic treatment.

On the basis of the various analyses, the following model for nanocaterpillar formation is proposed. As the PA block grows to a certain size (Figure 4a), the produced diblock copolymer initially self-assembles into spheres, as expected (Figure 4b). As additional COT diffuses into the core, it expands until the PN shell block can no longer solvate the PA core as spheres (Figure 4c). This exposed PA core in the sphere then spontaneously clings to other spheres with extended PA cores (Figure 4d) forming the final nanocaterpillar by strong $\pi-\pi$ interactions to minimize the area of solvophobic PA cores (Figure 4e). This

dx.doi.org/10.1021/ja305150c | J. Am. Chem. Soc. 2012, 134, 14291–14294

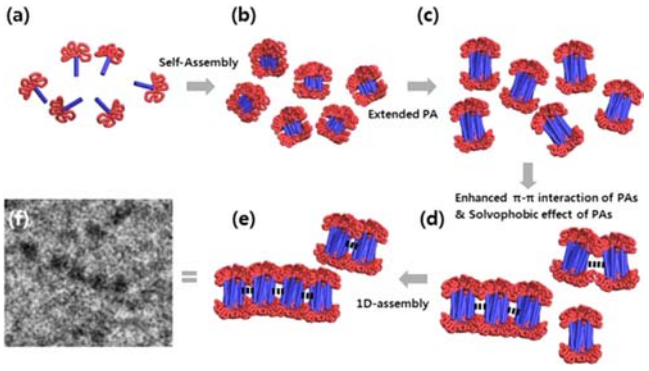

Figure 4. Proposed mechanism for in situ nanoparticlization of PN-*b*-PA into nanocaterpillars (INCP).

model is in excellent agreement with the observations that the larger DP of the PA core block induced only moderate increase in heights of the nanocaterpillars, but huge increases in their hydrodynamic volumes and molecular weights (Figure S5). Typical wormlike micelles were previously formed by the fusion of multiple spherical micelles[1] or elongation from seed micelles.[4] However, these nanocaterpillars with totally separated cores are uniquely shaped by individually isolated spheres that form loose contacts with others (Figure 4f). This unique assembly is markedly different from a conventional self-assembly of block copolymers consisting of flexible segments because the rigid and immobile conjugated PA core cannot fuse together to form the typical cylinders. Nevertheless, the long PA segments are held tight by $\pi-\pi$ interactions that are strong enough to endure heat and mechanical force. Lastly, this nanostructure in which the core is protected by the shell explains why the nanocaterpillars are stable in solution and in air with a deep HOMO level while pristine PA is unstable under these conditions.

In summary, we have synthesized a soluble and stable PA-based BCP by using the third-generation Grubbs catalyst to achieve ROMP of COT without severe depolymerization that releases benzene. Amazingly, this simple PN-*b*-PA formed nanocaterpillar supramolecules in a variety of solvents by direct and mild synthesis. These results demonstrate that a unique self-assembled nanostructure formed by the in situ nanoparticlization of conjugated polymer (INCP) method[15] could provide a novel strategy to protect rather unstable semiconducting PA, thus allowing the nanowires to be used in nanoelectronic applications.

■ ASSOCIATED CONTENT

Ⓢ Supporting Information

Experimental details and further characterization. This material is available free of charge via the Internet at http://pubs.acs.org.

■ AUTHOR INFORMATION

Corresponding Author

tlc@snu.ac.kr

Notes

The authors declare no competing financial interest.

■ ACKNOWLEDGMENTS

T.-L.C. dedicates this paper to Prof. Myongsoo Lee for his outstanding contribution to the chemistry of self-assembly at SNU. Financial support from the National Research Foundation of MEST, Korea, and the BRL is acknowledged. We thank Jeong-Hee Kim (Polymeric and Soft Nanomaterial Lab, SNU) and NCIRF at SNU for generous support of the TEM and EA experiments and helpful discussions. E.L. thanks the 2009 University–Institute Cooperation Program at CNU.

■ REFERENCES

(1) (a) Cui, H.; Chen, Z.; Zhong, S.; Wooley, K. L.; Pochan, D. J. *Science* **2007**, *317*, 647. (b) Li, Z.; Ma, J.; Lee, N. S.; Wooley, K. L. *J. Am. Chem. Soc.* **2011**, *133*, 1228. (c) Jain, S.; Bates, F. S. *Science* **2003**, *300*, 460. (d) Ma, Q.; Remsen, E. E.; Clark, C. G.; Kowalewski, T.; Wooley, K. L. *Proc. Natl. Acad. Sci. U.S.A.* **2002**, *99*, 5058.

(2) Yin, L.; Hillmyer, M. A. *Macromolecules* **2011**, *44*, 3021.

(3) (a) Moughton, A. O.; Hillmyer, M. A.; Lodge, T. P. *Macromolecules* **2011**, *45*, 2. (b) Li, Z.; Kesselman, E.; Talmon, Y.; Hillmyer, M. A.; Lodge, T. P. *Science* **2004**, *306*, 98. (c) Gröschel, A. H.; Schacher, F. H.; Schmalz, H.; Borisov, O. V.; Zhulina, E. B.; Walther, A.; Müller, A. H. E. *Nat. Commun.* **2012**, *3*, 710.

(4) (a) Gilroy, J. B.; Gädt, T.; Whittell, G. R.; Chabanne, L.; Mitchels, J. M.; Richardson, R. M.; Winnik, M. A.; Manners, I. *Nat. Chem.* **2010**, *2*, 566. (b) Xiaosong, W.; Guerin, G.; Hal, W.; Yishan, W.; Manners, I.; Winnik, M. A. *Science* **2007**, *317*, 644. (c) Patra, S. K.; Ahmed, R.; Whittell, G. R.; Lunn, D. J.; Dunphy, E. L.; Winnik, M. A.; Manners, I. *J. Am. Chem. Soc.* **2011**, *133*, 8842.

(5) Bhargava, P.; Tu, Y.; Zheng, J. X.; Xiong, H.; Quirk, R. P.; Cheng, S. Z. D. *J. Am. Chem. Soc.* **2007**, *129*, 1113.

(6) (a) Li, Y.; Armes, S. P. *Angew. Chem., Int. Ed.* **2010**, *49*, 4042. (b) Sugihara, S.; Blanazs, A.; Armes, S. P.; Ryan, A. J.; Lewis, A. L. *J. Am. Chem. Soc.* **2011**, *133*, 15707. (c) Blanazs, A.; Madsen, J.; Battaglia, G.; Ryan, A. J.; Armes, S. P. *J. Am. Chem. Soc.* **2011**, *133*, 16581. (d) Charleux, B.; Delaittre, G.; Rieger, J.; D'Agosto, F. *Macromolecules* **2012**, DOI: 10.1021/ma300713f.

(7) (a) Shirakawa, H. *Angew. Chem., Int. Ed.* **2001**, *40*, 2574. (b) Etemad, S.; Heeger, A. *Annu. Rev. Phys. Chem.* **1982**, *33*, 443.

(8) (a) Klavetter, F. L.; Grubbs, R. H. *J. Am. Chem. Soc.* **1988**, *110*, 7807. (b) Scherman, O. A.; Grubbs, R. H. *Synth. Met.* **2001**, *124*, 431.

(9) (a) Edwards, J. H.; Feast, W. J. *Polymer* **1980**, *21*, 595. (b) Swager, T. M.; Dougherty, D. A.; Grubbs, R. H. *J. Am. Chem. Soc.* **1988**, *110*, 2973. (c) Wu, C.; Niu, A.; Leung, L. M.; Lam, T. *J. Am. Chem. Soc.* **1999**, *121*, 1954.

(10) (a) Scherman, O. A.; Rutenberg, I. M.; Grubbs, R. H. *J. Am. Chem. Soc.* **2003**, *125*, 8515. (b) Mahmoud, A. *Synth. Met.* **1986**, *13*, 87.

(11) (a) Craig, G. S. W.; Cohen, R. E.; Schrock, R. R.; Esser, A.; Schrof, W. *Macromolecules* **1995**, *28*, 2512. (b) Krouse, S. A.; Schrock, R. R. *Macromolecules* **1988**, *21*, 1885.

(12) (a) Choi, T.-L.; Grubbs, R. H. *Angew. Chem., Int. Ed.* **2003**, *42*, 1743. (b) Kang, E.-H.; Lee, I. S.; Choi, T.-L. *J. Am. Chem. Soc.* **2011**, *133*, 11904.

(13) Yoshino, K. *Synth. Met.* **1989**, *28*, 669.

(14) Kaner, R. B.; Porter, S. J.; Nairns, D. P.; MacDiarmid, A. G. *J. Chem. Phys.* **1989**, *90*, 5102.

(15) Kim, J.; Kang, E.-H.; Choi, T.-L. *ACS Macro Lett.* **2012**, *1*, 1090.